

Effects due to two temperature and hall current in a nonlocal isotropic magneto-thermoelastic solid with memory dependent derivatives

Parveen Lata^{1a} and Sukhveer Singh^{*2}

¹Department of Basic and Applied Sciences, Punjabi University Patiala, India

²Punjabi University APS Neighbourhood Campus, Dehla Seehan, India

(Received May 29, 2021, Revised July 8, 2021, Accepted July 9, 2021)

Abstract. The paper is devoted to the study of thermomechanical interactions in a homogeneous nonlocal magneto-thermoelastic rotating medium under the effect of hall current and two temperature with memory dependent derivatives. A two-dimensional model has been assumed. Laplace and Fourier transforms have been used to find the solution to the problem in transformed domain. The analytical expressions of components of displacement, stress and current density and conductive temperature are obtained in the transformed domain. Numerical inversion technique has been applied to obtain the results in the physical domain and the results are depicted graphically to show the effect of nonlocal parameter on the components of displacements, stresses, current density and conductive temperature. The effect of nonlocal parameter and hall current parameter has been represented graphically by taking different values.

Keywords: hall current; memory dependent derivatives; nonlocality; rotation; stress components; thermoelasticity

1. Introduction

Hall current is produced due to the combined effect of electric and magnetic field in a conductor. Such conductors which exhibit this phenomenon are termed as Magneto-thermoelastic materials. These materials are very important due to their wide range of applications in the fields of geophysics, nuclear fields, seismology, inspecting materials, magnetometers and various other related fields. Nonlocal theory of thermoelasticity and two temperature theory of thermoelasticity are very important theories

The concept of two temperature was formulated by Chen and Gurtin (1968). They gave the concept of two temperature i.e., conductive temperature and thermodynamical temperature. Edelen and Laws (1971) and Edelen *et al.* (1971) gave the theory of nonlocal continuum mechanics which considers that the state of stress at a point of a body is a function of state of strains of all the points of the body. Marin (1996) discussed generalized solutions in elasticity of micropolar bodies with voids. Eringen (2002) gave and explored the Nonlocal Continuum Theories. Youssef (2006)

*Corresponding author, Assistant Professor, E-mail: sukhveer_17@pbi.ac.in

^aAssociate Professor, E-mail: parveenlata@pbi.ac.in

proposed a theory of two-temperature-generalized thermoelasticity and obtained the uniqueness theorem. Youssef and Al-Lehaibi (2007) estimated the effects of two temperature parameter in generalized thermoelasticity. Abbas *et al.* (2011) discussed generalized magneto-thermoelasticity in a fiber-reinforced anisotropic half-space. Othman and Abbas (2011) studied the effects of rotation on plane waves. Othman and Abbas (2012) proposed a generalized thermoelasticity of thermal-shock problem. Atwa and Jahangir (2014) investigated two temperature effects on a thermo-microstretch elastic solid. A model based upon two temperature generalized thermoelastic theory was proposed by Abbas (2014). Marin *et al.* (2015) discussed the considerations on double porosity structure for micropolar bodies. Sharma *et al.* (2016) investigated the thermomechanical interactions in transversely isotropic magneto-thermoelastic medium with two temperature. Alzahrani and Abbas (2016) studied the effect of magnetic field on a thermoelastic material under GN-III theory.

Ezzat and El-Barry (2017a, 2017b) studied magneto-thermoelastic materials with phase-lag and memory dependent derivatives. Bellifa *et al.* (2017) derived a nonlocal shear deformation theory while Karami *et al.* (2018) derived nonlocal strain gradient theory. Mokhtar *et al.* (2018) proposed a novel shear deformation theory based on nonlocal elasticity theory. Abouelregal (2019) presented a new nonlocal model based on Eringen's nonlocal elasticity and generalized thermoelasticity and studied magneto-thermoelastic waves. Abualnour *et al.* (2019) analyzed composite plates using a refined plate theory. Balubaid *et al.* (2019) studied free vibration of FG nanoscale plate. Belmahi *et al.* (2019) studied effects on the vibration of a nano beam using nonlocal elasticity theory. Benahmed *et al.* (2019) investigated nanoscale beam using nonlocal shear deformation theory. Soleimani *et al.* (2019) and Hussain *et al.* (2019) discussed nonlocal effect in their studies. Lata and Singh (2019) investigated the nonlocal effects under the effect of an inclined load on a thermoelastic solid. Khan *et al.* (2019) investigated magnetohydrodynamic fluid with variable thermal conductivity and chemical reaction over an exponentially stretching surface. Asghar *et al.* (2020) also studied the nonlocal effects in their studies and derived some important results and conclusions from their study. Saeed *et al.* (2020) gave a GL model on thermo-elastic interaction in a poroelastic material. Lata and Singh (2020a) studied the effects of hall current on a nonlocal magneto-thermoelastic solid due to a normal force and depicted the results graphically. Lata and Singh (2020b, 2020c) investigated thermomechanical interactions in nonlocal thermoelastic solid with two temperatures and with memory dependent derivatives respectively. Tahir *et al.* (2021) studied the dispersion relations of wave propagation in a FGM plate. Mudhaffar *et al.* (2021) discussed the bending behavior of a FGM plate subjected to a hygro-thermo-mechanical load. Tahir *et al.* (2021) and Bakoura *et al.* (2021) studied the wave propagation and buckling analysis respectively in functionally graded plates. Refrafi (2020) used a novel shear deformation theory in their study of functionally graded sandwich plates. Lata and Singh (2020d) discussed ramp type effects on a nonlocal thermoelastic solid. Lata and Singh (2020e, 2021) studied the wave propagation in nonlocal magneto-thermoelastic solids with Hall current and discussed the various effects on wave characteristics. Zhang *et al.* (2020) discussed Entropy impacts on the blood flow through anisotropically tapered arteries filled with magnetic zinc-oxide (ZnO) nanoparticles Lata and Singh (2020) discussed time harmonic interactions in nonlocal thermoelastic solid. Zenkour (2020) proposed a refined multi-dual-phase-lag model.

In this research paper, an attempt has been made to study the thermomechanical interactions in a homogeneous nonlocal magneto-thermoelastic rotating medium under the combined effect of hall current and two temperature parameter with the help of memory dependent derivatives. The effect of nonlocal parameter and hall current parameter has been represented graphically by taking

different values. The results might be useful for the scientists and researchers working for the development of nonlocal thermoelasticity and magneto-thermoelastic theories and related fields.

2. Basic equations

Following Eringen (2002) and Abouelregal (2019), the invariant form of nonlocal equation of motion can be written as follows

$$t_{ij,j} + (1 - \epsilon^2 \nabla^2) \vec{F}_i = \rho(1 - \epsilon^2 \nabla^2) [\vec{u} + \vec{\Omega} \times (\vec{\Omega} \times \vec{u}) + 2\vec{\Omega} \times \vec{u}]_i. \tag{1}$$

It is assumed that the homogeneous nonlocal isotropic magneto-thermoelastic solid is rotating with a uniform angular velocity $\vec{\Omega} = \Omega \hat{n}$, where \hat{n} is a unit vector demonstrating the direction of the rotation axis and $\vec{F}_i = \mu_0 (\vec{J} \times \vec{H}_0)_i$ denotes the Lorentz force, \vec{H}_0 is the external applied magnetic field intensity vector, \vec{J} is the current density vector, \vec{u} is the displacement vector, μ_0 and ϵ_0 are the magnetic and electric permeabilities respectively. The terms $\vec{\Omega} \times (\vec{\Omega} \times \vec{u})$ and $2\vec{\Omega} \times \vec{u}$ denote centripetal acceleration due to the time-varying motion and Coriolis acceleration respectively.

The above equations are supplemented by generalized Ohm's law for media with finite conductivity and including the hall current effect (from Kumar *et al.* (2017))

$$\vec{J} = \frac{\sigma_0}{1+m^2} \left(\vec{E} + \mu_0 \left(\vec{u} \times \vec{H} - \frac{1}{en_e} \vec{J} \times \vec{H}_0 \right) \right) \tag{2}$$

where, σ_0 is the electrical conductivity, $m (= \omega_e t_e)$ is the Hall parameter, ω_e is the electronic frequency, t_e is the electron collision time, e is the charge of an electron, n_e is the number of density of electrons.

Following Sarkar *et al.* (2018), the heat conduction equation with memory dependent derivatives and constitutive relations in a homogeneous nonlocal thermoelastic solid with two temperatures are given by

$$K^* \nabla^2 \varphi = \rho C^* \frac{\partial \theta}{\partial t} + \beta \theta_0 \frac{\partial}{\partial t} (\nabla \cdot u) + \int_{t-\tau}^t K(t-\xi) \left(\rho C^* \frac{\partial^2 \theta}{\partial \xi^2} + \beta \theta_0 \frac{\partial^2}{\partial \xi^2} (\nabla \cdot u) \right) d\xi, \tag{3}$$

where, $\theta = (1 - a \nabla^2) \varphi$,

$$(1 - \epsilon^2 \nabla^2) t_{ij} = \lambda u_{k,k} \delta_{ij} + \mu (u_{i,j} + u_{j,i}) - \beta T \delta_{ij}. \tag{4}$$

where λ, μ are Lamé's constants, ϵ is the nonlocal parameter, ρ is the mass density, $\vec{u} = (u, v, w)$ is the displacement vector, φ is the conductive temperature, a is two temperature parameter, θ is absolute temperature and θ_0 is reference temperature, K^* denotes the coefficient of the thermal conductivity, C^* the specific heat at constant strain, β is the thermal tensor and $\beta = (3\lambda + 2\mu)\alpha$ where α is coefficient of linear thermal expansion, e_{ij} are components of strain tensor, e_{kk} is the dilatation, δ_{ij} is the Kronecker delta, t_{ij} are the components of stress tensor.

3. Formulation of the problem

We consider a perfectly conducting homogeneous nonlocal isotropic magneto-thermoelastic

medium rotating uniformly with an angular velocity $\vec{\Omega}$ initially at uniform temperature T_0 . The rectangular Cartesian coordinate system (x, y, z) is introduced, having origin on the surface ($z=0$) with z -axis pointing normally downwards into the half space. For two-dimensional problem in xz -plane, we consider

$$\vec{u} = (u, 0, w). \quad (5)$$

$$\text{We also assume that } \vec{E} = (E_1, 0, E_3), \vec{\Omega} = (0, \Omega, 0). \quad (6)$$

Now, using Eq. (5)

$$J_y = 0 \quad (7)$$

The current density components J_x and J_z using Eq. (2) are given as

$$J_x = \frac{\sigma_0 \mu_0 H_0}{1+m^2} \left(m \frac{\partial u}{\partial t} - \frac{\partial w}{\partial t} \right), \quad (8)$$

$$J_z = \frac{\sigma_0 \mu_0 H_0}{1+m^2} \left(\frac{\partial u}{\partial t} + m \frac{\partial w}{\partial t} \right). \quad (9)$$

Using Eq. (5) in Eq. (1) and Eq. (3), yields

$$\begin{aligned} (\lambda + 2\mu) \frac{\partial^2 u}{\partial x^2} + (\lambda + \mu) \frac{\partial^2 w}{\partial x \partial z} + \mu \frac{\partial^2 u}{\partial z^2} - \beta \frac{\partial T}{\partial x} - (1 - \epsilon^2 \nabla^2) \mu_0 J_z H_0 \\ = \rho(1 - \epsilon^2 \nabla^2) \left\{ \frac{\partial^2 u}{\partial t^2} - \Omega^2 u + 2\Omega \frac{\partial w}{\partial t} \right\}, \end{aligned} \quad (10)$$

$$\begin{aligned} (\lambda + 2\mu) \frac{\partial^2 w}{\partial z^2} + (\lambda + \mu) \frac{\partial^2 u}{\partial x \partial z} + \mu \frac{\partial^2 w}{\partial z^2} - \beta \frac{\partial T}{\partial z} - (1 - \epsilon^2 \nabla^2) \mu_0 J_x H_0 \\ = \rho(1 - \epsilon^2 \nabla^2) \left\{ \frac{\partial^2 w}{\partial t^2} - \Omega^2 w - 2\Omega \frac{\partial u}{\partial t} \right\}, \end{aligned} \quad (11)$$

$$K^* \nabla^2 \varphi = \rho C^* \frac{\partial \theta}{\partial t} + \beta \theta_0 \frac{\partial}{\partial t} (\nabla \cdot u) + \int_{t-\tau}^t K(t-\xi) \left(\rho C^* \frac{\partial^2 \theta}{\partial \xi^2} + \beta \theta_0 \frac{\partial^2}{\partial \xi^2} (\nabla \cdot u) \right) d\xi. \quad (12)$$

Following Sarkar *et al.* (2018), the kernel function form is chosen as

$$K(t-\xi) = 1 - \frac{2b}{\omega}(t-\xi) + \frac{a^2}{\omega^2}(t-\xi)^2 = \begin{cases} 1 & \text{if } a = 0, b = 0 \\ 1 - \frac{(t-\xi)}{\omega} & \text{if } a = 0, b = \frac{1}{2} \\ 1 - (t-\xi) & \text{if } a = 0, b = \frac{\omega}{2} \\ \left(1 - \frac{t-\xi}{\omega}\right)^2 & \text{if } a = b = 1 \end{cases} \quad (13)$$

we define the following dimensionless quantities

$$\begin{aligned} (x', z', u', w') = \frac{\omega_1}{c_1} (x, z, u, w), \quad t'_{ij} = \frac{t_{ij}}{\beta \theta_0}, \quad t' = \omega_1 t, \quad a' = \frac{\omega_1^2}{c_1^2} a, \\ T' = \frac{T}{T_0}, \Omega' = \frac{\Omega}{\omega_1}, \tau'_v = \omega_1 \tau_v, \tau'_0 = \omega_1 \tau_0, \tau'_q = \omega_1 \tau_q. \end{aligned} \quad (14)$$

where, $c_1^2 = \frac{\mu}{\rho}$ and $\omega_1 = \frac{\rho C^* c_1^2}{K^*}$.

The relations between non-dimensional displacement components u, w and the dimensionless potential functions q, ψ can be expressed as

$$u = \frac{\partial q}{\partial x} - \frac{\partial \psi}{\partial z}, \quad w = \frac{\partial q}{\partial z} + \frac{\partial \psi}{\partial x} \tag{15}$$

Upon introducing the quantities defined by Eq. (14) and (15) in Eqs. (10)-(12), and suppressing the primes, yields

$$\left\{ (1 + a_1)\nabla^2 - (1 - \epsilon^2\nabla^2) \left[\frac{M}{1+m^2} \frac{\partial}{\partial t} + \frac{\partial^2}{\partial t^2} - a_3\Omega^2 \right] \right\} q - a_2(1 - a\nabla^2)\varphi = 0, \tag{16}$$

$$\left\{ \nabla^2 - (1 - \epsilon^2\nabla^2) \left(\frac{\partial^2}{\partial t^2} - a_3\Omega^2 \right) \right\} \psi = 0, \tag{17}$$

$$\nabla^2\varphi = (1 + \omega D_\omega)[a_3(1 - a\nabla^2) \frac{\partial \varphi}{\partial t} C^* \frac{\partial \theta}{\partial t} + a_4 \frac{\partial e}{\partial t}], \tag{18}$$

where, $a_1 = \frac{\lambda+\mu}{\mu}$, $a_2 = \frac{\beta\theta_0}{\mu}$, $a_3 = \frac{\omega_1^2}{c_1^2}$, $a_4 = \frac{\rho C^* c_1^2}{K^* \omega_1}$, $a_5 = \frac{\beta c_1^2}{K^* \omega_1}$ and $M = \frac{\sigma_0 \mu_0^2 H_0^2}{\rho}$.

The initial and regularity conditions are given by

$$\begin{aligned} u_1(x, z, 0) = 0 = \dot{u}(x, z, 0), \\ w(x, z, 0) = 0 = \dot{w}(x, z, 0), \\ \varphi(x, z, 0) = 0 = \dot{\varphi}(x, z, 0) \text{ for } z \geq 0, -\infty < x < \infty, \\ u(x, z, t) = w(x, z, t) = \varphi(x, z, t) = 0 \text{ for } t > 0 \text{ when } z \rightarrow \infty. \end{aligned}$$

Applying Laplace and Fourier Transform defined by

$$\bar{f}(x, z, s) = \int_0^\infty f(x, z, t) e^{-st} dt, \tag{19}$$

$$\hat{f}(\xi, z, s) = \int_{-\infty}^\infty \bar{f}(x, z, s) e^{i\xi x} dx. \tag{20}$$

on Eqs. (16)-(18), we obtain a system of equations

$$[(\delta_6 + \epsilon^2\delta_1)D^2 - (\delta_6\xi^2 + \delta_1\delta_3)]\bar{q} - [a_2(\delta_5 - aD^2)]\bar{\varphi} = 0, \tag{21}$$

$$[(1 + \epsilon^2\delta_2)D^2 - \xi^2 + \delta_2\delta_3]\bar{\psi} = 0, \tag{22}$$

$$[a_5\delta_4(D^2 - \xi^2)]\bar{q} + [a_4\delta_4\delta_5 + \xi^2 - (aa_4\delta_4 + 1)D^2]\bar{\varphi} = 0. \tag{23}$$

where, $\delta_1 = \frac{M}{1+m^2}s + s^2 - a_3\Omega^2$, $\delta_2 = s^2 - a_3\Omega^2$, $\delta_3 = 1 + \epsilon^2\xi^2$, $\delta_4 = s(1 + G)$, $\delta_5 = 1 + a\xi^2$, $\delta_6 = 1 + a_1$.

Also

$$G(s) = (1 - e^{-s\omega}) \left(1 - \frac{2b}{s\omega} + \frac{2a^2}{s^2\omega^2} \right) - e^{-s\omega} \left(a^2 - 2b + \frac{2a^2}{s\omega} \right) \tag{24}$$

where, a, b are constants such that

$$L(\omega D_\omega f(t)) = \begin{cases} 1 - e^{-s\omega} & \text{if } a = 0, b = 0 \\ 1 - \frac{(1-e^{-s\omega})}{s\omega} & \text{if } a = 0, b = \frac{1}{2} \\ (1 - e^{-s\omega}) - \frac{1}{s}(1 - e^{-s\omega}) + \omega e^{-s\omega} & \text{if } a = 0, b = \frac{\omega}{2} \\ \left(1 - \frac{2}{s\omega} \right) + \frac{2(1-e^{-s\omega})}{s^2\omega^2} & \text{if } a = b = 1 \end{cases} \tag{25}$$

From Eq. (21)-(23), we obtain a set of homogeneous equations which will have a nontrivial solution if determinant of coefficient $[\bar{q}, \bar{\varphi}, \bar{\psi}]^T$ vanishes so as to give a characteristic equation as

$$[D^6 + QD^4 + RD^2 + S](\bar{q}, \bar{\varphi}, \bar{\psi}) = 0. \tag{26}$$

where,

$$Q = \frac{1}{p} \{ [\delta_8 \delta_{10} \delta_{11} + \delta_7 (\delta_{10} \delta_{12} + \delta_9 \delta_{11} + \xi^2 \delta_{11})] + a_2 a_5 \delta_4 (\delta_5 \delta_{11} + a^2 \delta_{12} + a \xi^2 \delta_{11}) \},$$

$$R = \frac{-1}{p} \{ [\delta_7 \delta_{12} (\delta_9 + \xi^2) + \delta_8 (\delta_{10} \delta_{12} + \delta_9 \delta_{11} + \xi^2 \delta_{11})] + a_2 a_5 \delta_4 (\delta_5 \delta_{12} + \xi^2 \delta_5 \delta_{11} + a \xi^2 \delta_{12}) \},$$

$$S = \frac{1}{p} \{ \delta_8 \delta_{12} (\delta_9 + \xi^2) + a_2 a_5 \delta_4 \delta_5 \delta_{12} \xi^2 \},$$

$$P = \delta_{11} (\delta_7 \delta_{10} + a a_2 a_5 \delta_4),$$

$$D = \frac{d}{dz}.$$

The roots of Eq. (26) are $\pm \lambda_i (i = 1, 2, 3)$ satisfying the radiation condition that $\tilde{q}, \tilde{\varphi}, \tilde{\psi} \rightarrow 0$ as $z \rightarrow \infty$, the solutions of equation can be written as

$$\tilde{q} = A_1 e^{-\lambda_1 z} + A_2 e^{-\lambda_2 z} + A_3 e^{-\lambda_3 z}, \tag{27}$$

$$\tilde{\varphi} = d_1 A_1 e^{-\lambda_1 z} + d_2 A_2 e^{-\lambda_2 z} + d_3 A_3 e^{-\lambda_3 z}, \tag{28}$$

$$\tilde{\psi} = l_1 A_1 e^{-\lambda_1 z} + l_2 A_2 e^{-\lambda_2 z} + l_3 A_3 e^{-\lambda_3 z}. \tag{29}$$

where,

$$d_i = \frac{P^{**} \lambda_i^4 + Q^{**} \lambda_i^2 + R^{**}}{P^* \lambda_i^4 + Q^* \lambda_i^2 + R^*} \quad i = 1, 2, 3. \tag{30}$$

$$l_i = \frac{S^{**} \lambda_i^4 + T^{**} \lambda_i^2 + U^{**}}{P^* \lambda_i^4 + Q^* \lambda_i^2 + R^*} \quad i = 1, 2, 3. \tag{31}$$

$$P^* = -\delta_{10} \delta_{11}, \quad Q^* = \delta_{10} \delta_{12} + (\delta_9 + \xi^2) \delta_{11}, \quad R^* = -\delta_{12} (\delta_9 + \xi^2),$$

$$P^{**} = \delta_7 \delta_{11}, \quad Q^{**} = -\delta_7 \delta_{12} + \delta_8 \delta_{11}, \quad R = \delta_8 \delta_{12},$$

$$S^{**} = -(\delta_7 \delta_{10} + a a_2 \delta_5), \quad T^{**} = (\delta_9 + \xi^2) \delta_7 + \delta_8 \delta_{10} + a_2 a_5 (\delta_5 + \xi^2) \delta_4, \quad U^{**} = -(\delta_9 + \xi^2) \delta_8 + a_2 a_5 \delta_4 \delta_5 \xi^2.$$

4. Applications

On the half-space ($z = 0$) normal point force and thermal point source are applied. The boundary conditions are

$$(1) t_{zz}(x, z, t) = -F_1 \psi_1(x) \delta(t), \tag{32}$$

$$(2) t_{zx}(x, z, t) = 0, \tag{33}$$

$$(3) \frac{\partial}{\partial z} \varphi(x, z, t) = F_2 \psi_2(x) \delta(t) \text{ at } z = 0. \tag{34}$$

where, F_1 is the magnitude of the force applied, F_2 is constant force applied on the boundary, $\psi_1(x)$ specify the source distribution function along x axis and $\psi_2(x)$ specify the source distribution function along z axis.

Using the dimensionless quantities defined by Eq. (14) and using Eqs. (4), (5), (15), (19), (20) and substituting values of $\tilde{q}, \tilde{\varphi}$ and $\tilde{\psi}$ from Eqs. (27)-(29), in Eqs. (32)-(34) and solving, we obtain the components of displacement, stress and conductive temperature as

$$\tilde{u} = \frac{F_1 \tilde{\psi}_1(\xi)}{s \Delta} \{ \sum_{i=1}^3 \eta_i (\iota \xi + \lambda_i l_i) e^{-\lambda_i z} \} + \frac{F_2 \tilde{\psi}_2(\xi)}{s \Delta} \{ \sum_{i=1}^3 \eta_{i+3} (\iota \xi + \lambda_i l_i) e^{-\lambda_i z} \}, \tag{35}$$

$$\tilde{w} = \frac{F_1 \tilde{\psi}_1(\xi)}{s\Delta} \left\{ \sum_{i=1}^3 \eta_i (\iota \xi l_i - \lambda_i) e^{-\lambda_i z} \right\} + \frac{F_2 \tilde{\psi}_2(\xi)}{s\Delta} \left\{ \sum_{i=1}^3 \eta_{i+3} (\iota \xi l_i - \lambda_i) e^{-\lambda_i z} \right\}, \quad (36)$$

$$\tilde{\phi} = \frac{F_1 \tilde{\psi}_1(\xi)}{s\Delta} \left\{ \sum_{i=1}^3 \eta_i d_i e^{-\lambda_i z} \right\} + \frac{F_2 \tilde{\psi}_2(\xi)}{s\Delta} \left\{ \sum_{i=1}^3 \eta_{i+3} d_i e^{-\lambda_i z} \right\}, \quad (37)$$

$$\begin{aligned} \tilde{t}_{zz} = & \frac{-F_1 \tilde{\psi}_1(\xi)}{s\Delta} \left\{ \sum_{i=1}^3 [(\lambda + 2\mu)(\iota \xi l_i - \lambda_i) \lambda_i + \beta d_i (1 + a\xi^2 - a\lambda_i^2)] \eta_i e^{-\lambda_i z} \right\} \\ & - \frac{F_2 \tilde{\psi}_2(\xi)}{s\Delta} \left\{ \sum_{i=1}^3 [(\lambda + 2\mu)(\iota \xi l_i - \lambda_i) \lambda_i + \beta d_i (1 + a\xi^2 - a\lambda_i^2)] \eta_{i+3} e^{-\lambda_i z} \right\}, \end{aligned} \quad (38)$$

$$\begin{aligned} \tilde{t}_{zz} = & \frac{F_1 \tilde{\psi}_1(\xi)}{s\Delta} \left\{ \sum_{i=1}^3 \mu [\iota \xi (\iota \xi l_i - \lambda_i) - \lambda_i (\iota \xi + \lambda_i l_i)] \eta_i e^{-\lambda_i z} \right\} \\ & + \frac{F_2 \tilde{\psi}_2(\xi)}{s\Delta} \left\{ \sum_{i=1}^3 \mu [\iota \xi (\iota \xi l_i - \lambda_i) - \lambda_i (\iota \xi + \lambda_i l_i)] \eta_{i+3} e^{-\lambda_i z} \right\}, \end{aligned} \quad (39)$$

$$\begin{aligned} \tilde{t}_{xx} = & \frac{F_1 \tilde{\psi}_1(\xi)}{s\Delta} \left\{ \sum_{i=1}^3 [\iota \xi (\lambda + 2\mu)(\iota \xi + \lambda_i l_i) + \beta d_i (1 + a\xi^2 - a\lambda_i^2)] \eta_i e^{-\lambda_i z} \right\} \\ & + \frac{F_2 \tilde{\psi}_2(\xi)}{s\Delta} \left\{ \sum_{i=1}^3 [\iota \xi (\lambda + 2\mu)(\iota \xi + \lambda_i l_i) + \beta d_i (1 + a\xi^2 - a\lambda_i^2)] \eta_{i+3} e^{-\lambda_i z} \right\}, \end{aligned} \quad (40)$$

$$\tilde{j}_x = \frac{F_1 \tilde{\psi}_1(\xi)}{\Delta} \left\{ \sum_{i=1}^3 A [m - d_i] \eta_i e^{-\lambda_i z} \right\} + \frac{F_2 \tilde{\psi}_2(\xi)}{\Delta} \left\{ \sum_{i=1}^3 A [m - d_i] \eta_{i+3} e^{-\lambda_i z} \right\}, \quad (41)$$

$$\tilde{j}_z = \frac{F_1 \tilde{\psi}_1(\xi)}{\Delta} \left\{ \sum_{i=1}^3 A [1 + m d_i] \eta_i e^{-\lambda_i z} \right\} + \frac{F_2 \tilde{\psi}_2(\xi)}{\Delta} \left\{ \sum_{i=1}^3 A [1 + m d_i] \eta_{i+3} e^{-\lambda_i z} \right\}, \quad (42)$$

$$\Delta = \eta_1 \Delta_{11} - \eta_2 \Delta_{12} + \eta_3 \Delta_{13}. \quad (43)$$

where,

$$\begin{aligned} \eta_1 = & \Delta_{22} \Delta_{33} - \Delta_{32} \Delta_{23}, \eta_2 = \Delta_{21} \Delta_{33} - \Delta_{31} \Delta_{23}, \eta_3 = \Delta_{21} \Delta_{32} - \Delta_{31} \Delta_{22}, \eta_4 = \Delta_{22} \Delta_{11} - \Delta_{12} \Delta_{21}, \\ \eta_5 = & \Delta_{23} \Delta_{11} - \Delta_{13} \Delta_{21}, \eta_6 = \Delta_{23} \Delta_{12} - \Delta_{13} \Delta_{22}, A = \frac{\sigma_0 \mu_0 H_0 s}{1 + m^2}, \\ \Delta_{1j} = & (\lambda + 2\mu) \lambda_j^2 - \iota \xi \lambda_j l_j + \beta d_j (a \lambda_j^2 - \delta_5), \Delta_{2j} = 2\iota \xi - l_j \xi^2 - \lambda_j^2 l_j, \Delta_{3j} = \lambda_j d_j; j = 1, 2, 3. \end{aligned}$$

5 Special cases

a. Mechanical force on the half-space surface:

Taking $F_2 = 0$ in Eqs. (35)-(42), we obtain the components of displacement, stress and conductive temperature due to mechanical force.

b. Thermal source on the half-spacesurface:

Taking $F_1 = 0$ in Eqs. (35)-(42), we obtain the components of displacement, stress and conductive temperature due to thermal force.

5.1 Concentrated force

The solution due to concentrated normal force and thermal point source on the half space is obtained by taking

$$\psi_1(x) = \delta(x), \psi_2(x) = \delta(x). \quad (44)$$

Applying Laplace and Fourier transform as defined by Eqs. (19)-(20), we obtain

$$\widehat{\psi}_1(\xi) = 1, \widehat{\psi}_2(\xi) = 1. \quad (45)$$

The expressions for displacement, stresses and conductive temperature can be obtained for concentrated normal force and thermal source by replacing $\widehat{\psi}_1(\xi)$ and $\widehat{\psi}_2(\xi)$ from Eq. (45) in Eqs. (35)-(42) respectively.

5.2 Uniformly distributed force

The solution due to uniformly distributed load applied on the half space is obtained by setting

$$\psi_1(x) = \psi_2(x) = \begin{cases} 1 & \text{if } |x| \leq m \\ 0 & \text{if } |x| > m \end{cases} \quad (46)$$

The Laplace and Fourier transform of $\psi_1(x)$ with respect to the pair (x, ξ) for the case of a uniform strip load of non-dimensional width $2m$ applied at origin of co-ordinate system $x = z = 0$ in the dimensionless form after suppressing the primes becomes

$$\widehat{\psi}_1(\xi) = \widehat{\psi}_2(\xi) = \left[2 \sin(\xi m) / \xi \right] \xi \neq 0. \quad (47)$$

The expressions for displacement, stresses and conductive temperature can be obtained for uniformly distributed normal force and thermal source by replacing $\widehat{\psi}_1(\xi)$ and $\widehat{\psi}_2(\xi)$ from Eq. (47) in Eqs. (35)-(42) respectively.

6. Particular cases

- If $a = 0$, then from Eqs. (35)-(42), the corresponding expressions for displacements, stresses, current density and conductive temperature for nonlocal isotropic magneto-thermoelastic solid without two temperature are obtained.
- If $\epsilon = 0$, then from Eqs. (35)-(42), the corresponding expressions for displacements, stresses, current density and conductive temperature for local isotropic magneto-thermoelastic solid with two temperature are obtained.
- If $\epsilon = a = 0$, then from Eqs. (35)-(42), the corresponding expressions for displacements, stresses, current density and conductive temperature for a local isotropic solid without two temperature are obtained.
- If $m = \epsilon = 0$, then from Eqs. (35)-(42), the corresponding expressions for displacements, stresses, current density and conductive temperature for a local isotropic solid without hall current are obtained.
- If $m = 0$, then from Eqs. (35)-(42), the corresponding expressions for displacements, stresses, current density and conductive temperature for a nonlocal isotropic solid without hall current are obtained.

7. Inversion of the transformation

To obtain the solution of the problem in physical domain, we need to invert the transforms in Eqs. (35)-(42). As the components of displacement, stress and current density and conductive

temperature are functions of the form $f(\xi, z, s)$. To obtain the function $f(x, z, t)$ in the physical domain, we invert the Fourier transform as used by Sharma *et al.* (2008), using

$$\tilde{f}(x, z, s) = \frac{1}{2\pi} \int_{-\infty}^{\infty} e^{-i\xi x} \hat{f}(\xi, z, s) d\xi = \frac{1}{2\pi} \int_{-\infty}^{\infty} |\cos(\xi x) f_e - i \sin(\xi x) f_0| d\xi . \quad (48)$$

where, f_e and f_0 are respectively the even and odd parts of $\hat{f}(\xi, z, s)$. Thus the expression (48) gives the Laplace transform $\tilde{f}(x, z, s)$ of the function $f(x, z, t)$. Following Honig and Hirdes, the Laplace transform function $\tilde{f}(x, z, s)$ can be inverted to $f(x, z, t)$.

The Last step is to calculate the integral in Eq. (48). The method used is as described by Press. It involves the use of Romberg's integration with adaptive step size.

8. Numerical results and discussion:

Magnesium material is chosen for the purpose of numerical calculation and according to Dhaliwal and Singh (1980), physical data for which is given as

$$\lambda = 9.4 \times 10^{10} Nm^{-2}, \mu = 3.278 \times 10^{10} Nm^{-2}, K^* = 1.7 \times 10^2 Wm^{-1}K^{-1}, \rho = 1.74 \times 10^3 Kgm^{-3}, \theta_0 = 298 K, C^* = 10.4 \times 10^2 JKg^{-1}deg^{-1}, \omega_1 = 3.58, a = 0.05.$$

A comparison of values of displacement components u and w , stress components t_{zz}, t_{xx}, t_{zx} , current density components J_x, J_z and conductive temperature φ for a nonlocal isotropic magneto-thermoelastic solid with distance x has been made for the local parameter ($\epsilon = 0$) and nonlocal parameter ($\epsilon = 1$) and Hall parameter ($m = 0$ and $m = 1$).

- 1) The solid red colored line with center symbol square corresponds to local parameter $\epsilon = 0$ and $m = 0$.
- 2) The solid blue colored line with center symbol star corresponds to local parameter $\epsilon = 0$ and $m = 1$.
- 3) The solid green colored line with center symbol circle corresponds to nonlocal parameter $\epsilon = 1$ and $m = 0$.
- 4) The solid purple colored line with center symbol triangle corresponds to nonlocal parameter $\epsilon = 1$ and $m = 1$.

8.1 Concentrated force

a) Mechanical force on the surface of half-space

Fig. 1, shows the variations in values of displacement component u under the effect of concentrated mechanical force. It is clear from the figure that the values of u follow oscillatory pattern. For $x \leq 6$, the variations for local parameter are less oscillatory as compared to nonlocal parameter but the difference in magnitude is less in the second half. Fig. 2 depicts the variation of values of displacement component w . The pattern is oscillatory with a visible difference between values for local and non-local parameters as well for Hall parameter. For $\epsilon = 1$ and $m = 1$, the oscillatory behavior is of less magnitude and magnitude follows a decreasing pattern as displacement increase. Fig. 3 and Fig. 4 describe the variations of stress components t_{zz} and t_{xx} with respect to displacement. For both local and non-local parameters, the behavior is oscillatory but the magnitude is more in case of nonlocal parameter. Fig. 5 shows the variation of stress component t_{zx} . In this case the trend followed is oscillatory but with more variations when the Hall parameter is non-zero. Fig. 6 illustrates the variation of conductive temperature φ . The

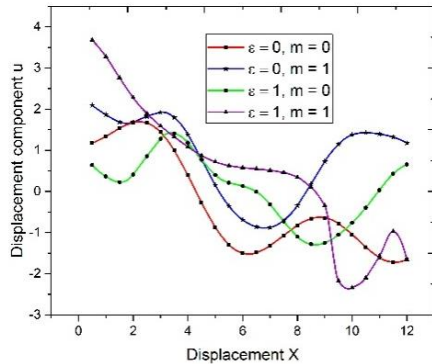


Fig. 1 Variation of displacement component u with displacement x (mechanical concentrated force)

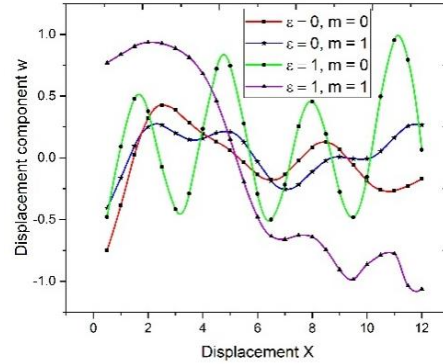


Fig. 2 Variation of displacement component w with displacement x (mechanical concentrated force)

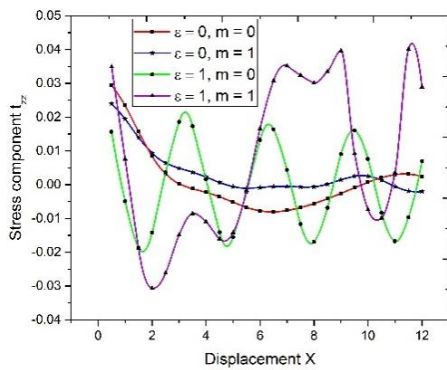


Fig. 3 Variation of stress component t_{zz} with displacement x (mechanical concentrated force)

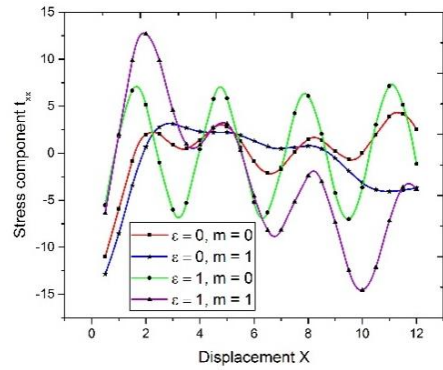


Fig. 4 Variation of stress component t_{xx} with displacement x (mechanical concentrated force)

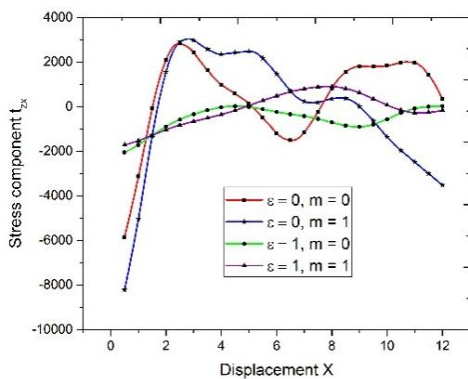


Fig. 5 Variation of stress component t_{zx} with displacement x (mechanical concentrated force)

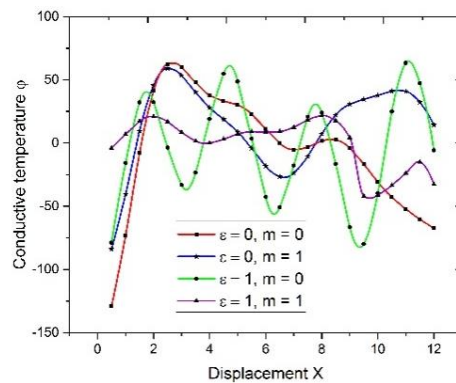


Fig. 6 Variation of conductive temperature ϕ with displacement x (mechanical concentrated force)

behavior followed is oscillatory. Fig. 7 and Fig. 8 show the variations of current density components J_x and J_z respectively. It is clear that the behavior is oscillatory in both. While, in case of J_x , the variations are of maximum magnitude in case of nonlocal parameter with Hall parameter

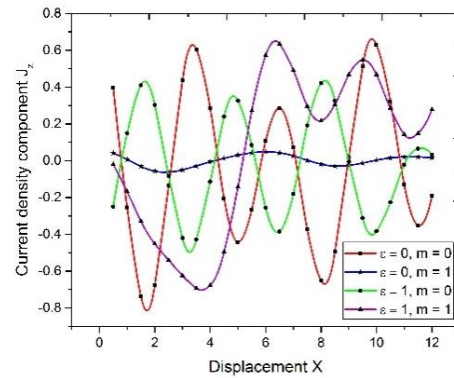
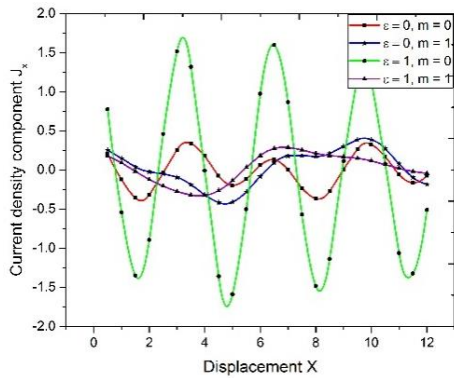


Fig. 7 Variation of current density component J_x with displacement x (mechanical concentrated force) Fig. 8 Variation of current density component J_z with displacement x (mechanical concentrated force)

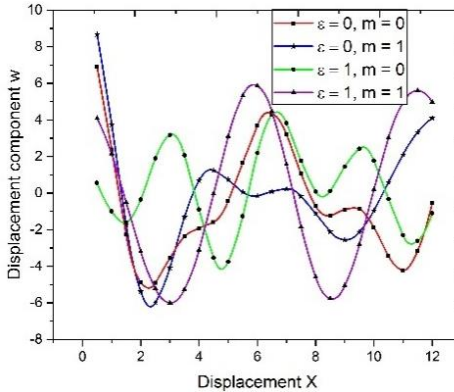
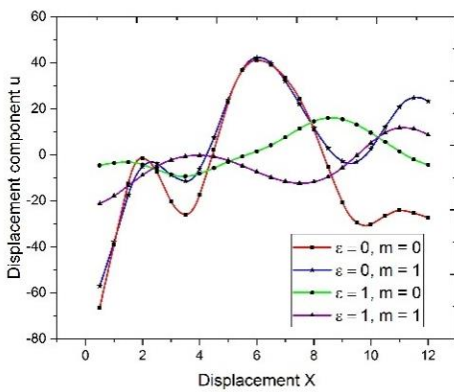


Fig. 9 Variation of displacement component u with displacement x (thermal concentrated force) Fig. 10 Variation of displacement component w with displacement x (thermal concentrated force)

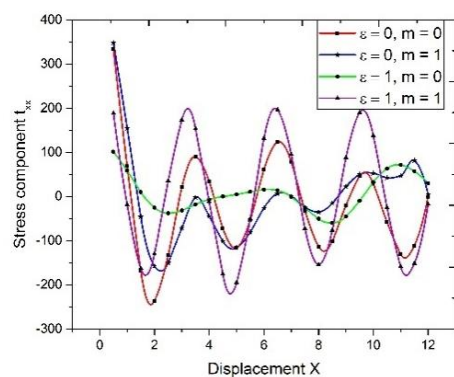
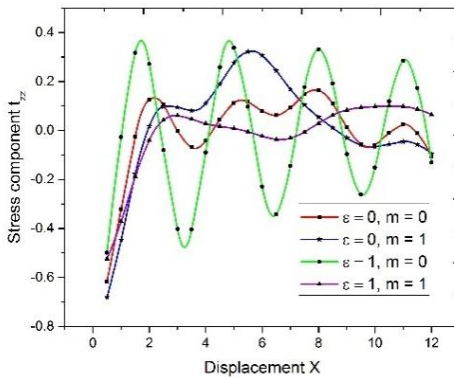


Fig. 11 Variation of stress component t_{zz} with displacement x (thermal concentrated force) Fig. 12 Variation of stress component t_{xx} with displacement x (thermal concentrated force)

as zero. In case of J_z , the variations are of minimum magnitude for local parameter with non-zero Hall parameter.

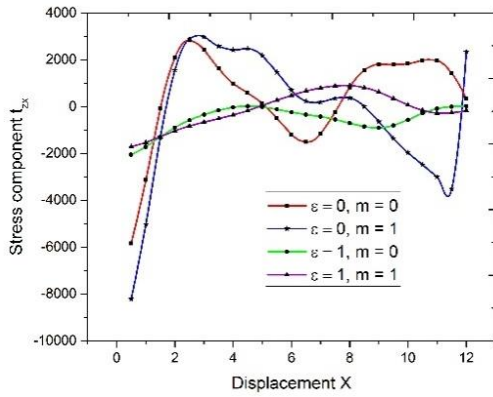


Fig. 13 Variation of stress component t_{zx} with displacement x (thermal concentrated force)

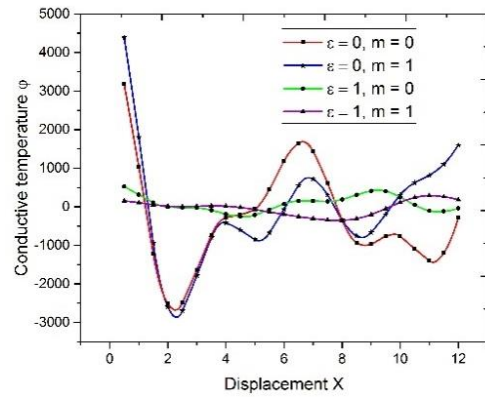


Fig. 14 Variation of conductive temperature ϕ with displacement x (thermal concentrated force)

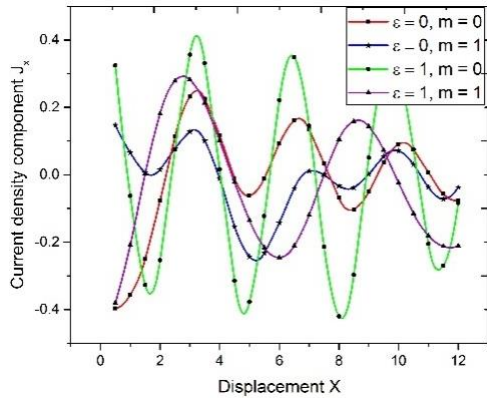


Fig. 15 Variation of current density component J_x with displacement x (thermal concentrated force)

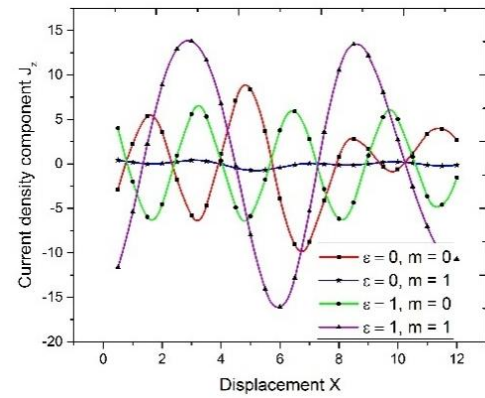


Fig. 16 Variation of current density component J_z with displacement x (thermal concentrated force)

b) Thermal source on the surface of half-space

Fig. 9 and Fig. 10, shows the variations in values of displacement components u and w respectively. The behavior followed is oscillatory for both. Non-locality and Hall effect are clearly causing the effects in variations. Fig. 11 depicts the variations of values of stress component t_{zz} . The behavior followed is oscillatory and the effects of non-local parameter and Hall parameter can be clearly noticed. Also, the magnitude of oscillations is of higher magnitude for local parameter with zero Hall parameter. Fig. 12 and Fig. 13 describes the variations of stress component t_{xx} and stress component t_{zx} respectively. Hall current and nonlocality both are clearly causing enough differences in variations. Fig. 14 shows the variation of conductive temperature ϕ . As per the trend, the variations are oscillatory with difference for local and non-local parameter values. Also, the variations decrease with nonlocal effect. Fig. 15 and Fig. 16 show the variations of current density components J_x and J_z respectively. The behavior is oscillatory in both the cases. The variations are there due to nonlocal parameter and Hall parameter. In case of J_z , the variations are of minimum magnitude for local parameter with Hall parameter.

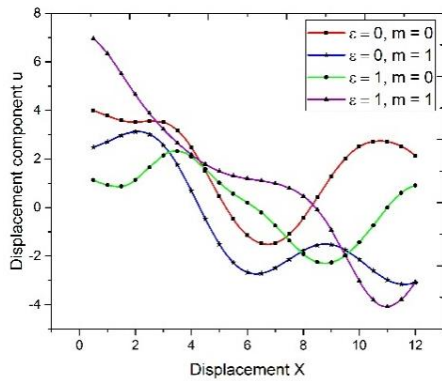


Fig. 17 Variation of displacement component u with displacement x (mechanical uniformly distributed force)

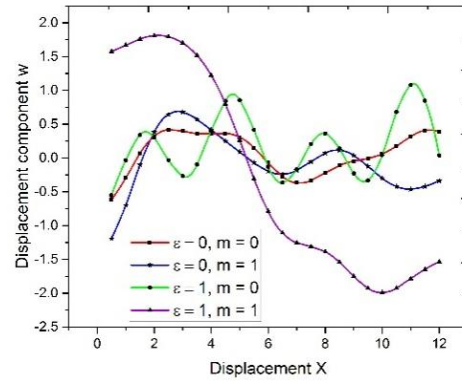


Fig. 18 Variation of displacement component w with displacement x (mechanical uniformly distributed force)

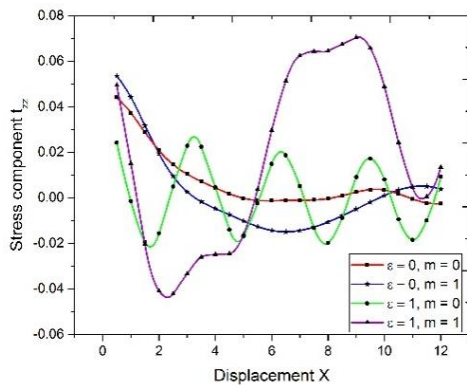


Fig. 19 Variation of stress component t_{zz} with displacement x (mechanical uniformly distributed force)

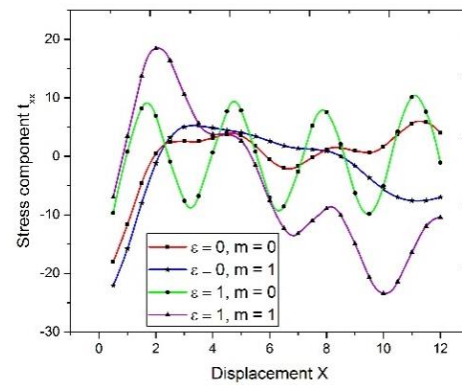


Fig. 20 Variation of stress component t_{xx} with displacement x (mechanical uniformly distributed force)

8.2 Uniformly distributed force

a) Mechanical force on the surface of half-space

Fig. 17 and Fig. 18, shows the variations in values of displacement component u and w respectively under the effect of concentrated mechanical force with respect to displacement. It is clear from the figures that the values follow an oscillatory pattern with a visible difference for both nonlocal and Hall parameter. In case of displacement component w , the variations for nonlocal parameter with Hall effect are less oscillatory and follows almost a decreasing pattern during the mid-path as compared to other values. Fig. 19 depicts the variation of values of stress component t_{zz} with respect to displacement. The pattern followed is oscillatory and the difference is there between values for local and non-local parameters as well for Hall parameter. For $\epsilon = 1$ and $m = 1$, the magnitude is maximum. Fig. 20 and Fig. 21 describe the variations of stress components t_{xx} and t_{zx} with respect to displacement. For both local and non-local parameters, the behavior is oscillatory. The magnitude is more in case of nonlocal parameter for t_{xx} , while the trend is

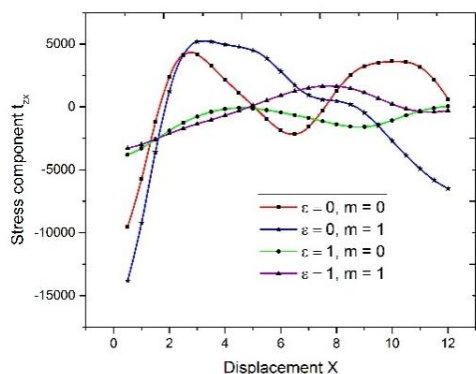


Fig. 21 Variation of stress component t_{zx} with displacement x (mechanical uniformly distributed force)

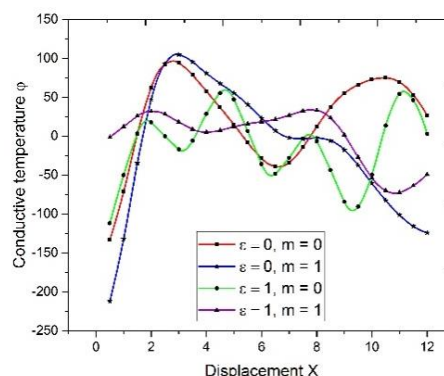


Fig. 22 Variation of conductive temperature φ with displacement x (mechanical uniformly distributed force)

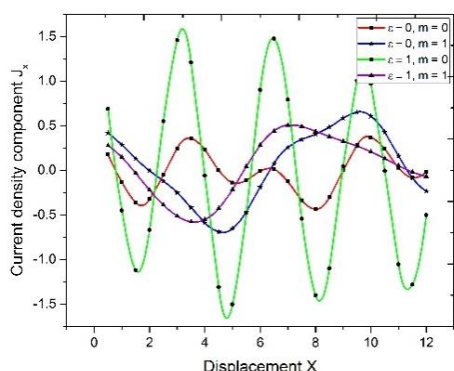


Fig. 23 Variation of current density component J_x with displacement x (mechanical uniformly distributed force)

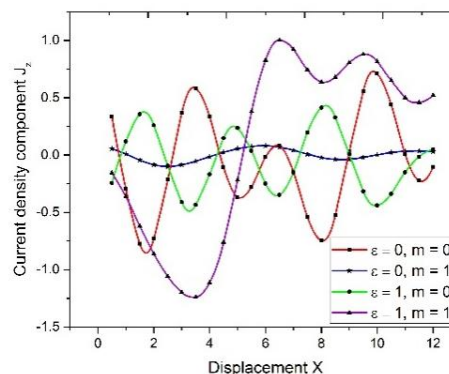


Fig. 24 Variation of current density component J_z with displacement x (mechanical uniformly distributed force)

in the case of stress component t_{zx} . Fig. 22 shows the variation of conductive temperature φ . The behavior is oscillatory as per the trend. The variations in magnitude are more for local parameter as compares to nonlocal parameter. Fig. 23 and Fig. 24 illustrates the variations of current density components J_x and J_z respectively. It is clear that the behavior is oscillatory in both. In case of J_x , the variations are of maximum magnitude in case of nonlocal parameter with Hall parameter as zero. While for J_z , the variations increase with Hall parameter.

b) Thermal source on the surface of half-space

Fig. 25 illustrates the variations in values of displacement component u . The behavior followed is oscillatory and the effect of nonlocal parameter and Hall parameter are clearly causing the effects in variations. The magnitude of variations is maximum for local parameter as compared to nonlocal parameter. Fig. 26 shows the variations in values of displacement component w , being oscillatory in nature with the effects of nonlocal parameter and Hall parameter causing the effects in variation. Fig. 27 depicts the variations of values of stress component t_{zz} . The behavior followed is oscillatory and the effects of non-local parameter and Hall parameter are clearly

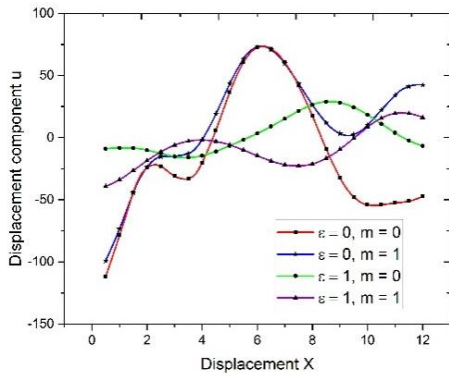


Fig. 25 Variation of displacement component u with displacement x (thermal uniformly distributed force)

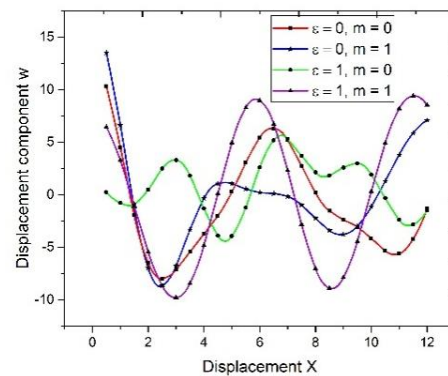


Fig. 26 Variation of displacement component w with displacement x (thermal uniformly distributed force)

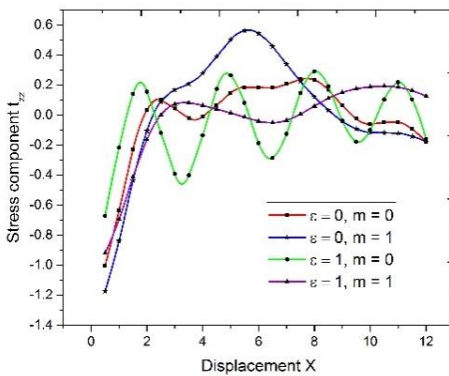


Fig. 27 Variation of stress component t_{zz} with displacement x (thermal uniformly distributed force)

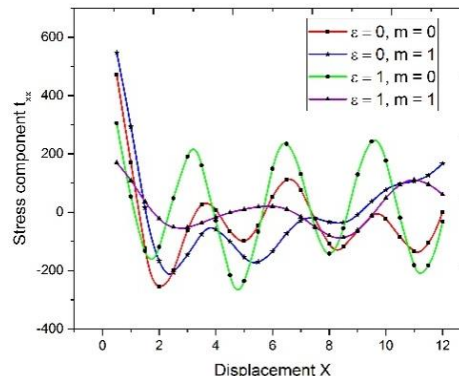


Fig. 28 Variation of stress component t_{xx} with displacement x (thermal uniformly distributed force)

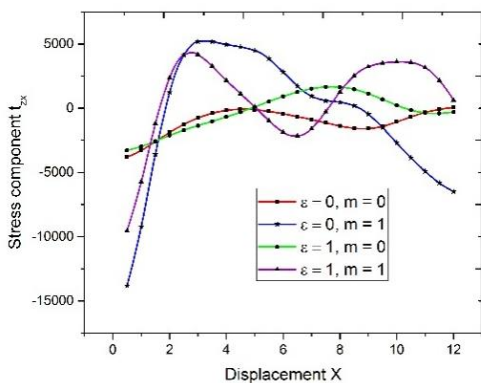


Fig. 29 Variation of stress component t_{zx} with displacement x (thermal uniformly distributed force)

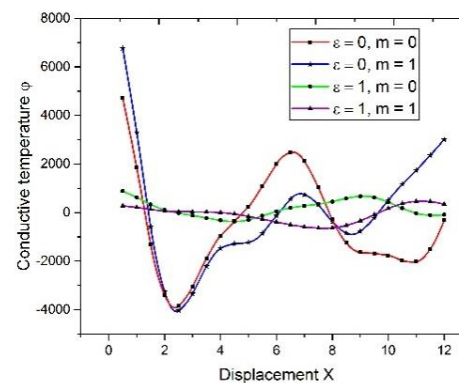


Fig. 30 Variation of conductive temperature ϕ with displacement x (thermal uniformly distributed force)

visible. Fig. 28 and Fig. 29 describes the variations of stress component t_{xx} and stress component t_{zx} respectively. The behavior followed is oscillatory. For stress component t_{xx} , the magnitude of

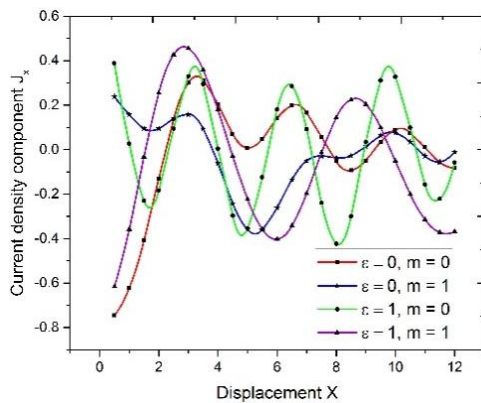


Fig. 31 Variation of current density component J_x with displacement x (thermal uniformly distributed force)

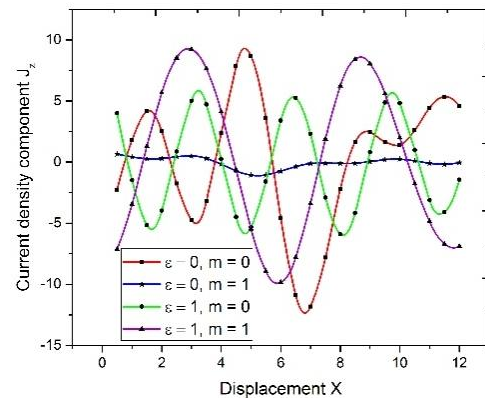


Fig. 32 Variation of current density component J_z with displacement x (thermal uniformly distributed force)

oscillations is comparatively more for nonlocal parameter without Hall effect while in case of stress component t_{zx} , the variations are less for local as well as nonlocal parameter without Hall parameter. Fig. 30 shows the variation of conductive temperature φ . As per the trend, the variations are oscillatory. Also, the variations of magnitude are less for nonlocal parameter. Fig. 31 and Fig. 32 show the variations of current density components J_x and J_z respectively. The behavior is oscillatory as per the trend and the variations are there due to Hall parameter and nonlocality. In case of J_z , the variations are of comparatively less in magnitude for local parameter with Hall parameter.

8. Conclusions

In the above discussion, the effects of Hall parameter and nonlocal parameter on the components of displacements, stresses, current density and conductive temperature have been examined and depicted graphically on a nonlocal thermo-elastic solid. It is clear that nonlocality and Hall effect are playing a significant effect on all the components. Results are illustrated in the forms of graphs using thermal and mechanical sources with two types of forces i.e., concentrated and uniformly distributed force. From graphs, it is observed that rotation and nonlocal parameter play a key role in the variations on various components. The results inspire us to study magneto-thermoelastic materials as an innovative domain of nonlocal isotropic thermoelastic solids. The shape of curves shows the impact of nonlocal and Hall parameter on the body. The outcomes of this research are extremely helpful in the 2-D problem with dynamic response of isotropic magneto-thermoelastic medium with rotation and nonlocality which can be beneficial in the fields of geophysics, geomagnetism, power plants, composite engineering, high-energy particle accelerators etc. It can also be helpful to the researchers working in the field of material engineering, marine engineering for the theoretical considerations of seismic sources and in the development of the theory of nonlocal magneto-thermoelasticity.

References

- Abbas, I.A. (2014), "A GN model based upon two temperature generalized thermoelastic theory in an unbounded medium with a spherical cavity", *Appl. Math. Comput.*, **245**, 108-115. <https://doi.org/10.1016/j.amc.2014.07.059>.
- Abbas, I.A., Abo-El-Nour, N. and Othman, M.I. (2011), "Generalized magneto-thermoelasticity in a fiber-reinforced anisotropic half-space", *Int. J. Thermophys.*, **32**(5), 1071-1085. <https://doi.org/10.1007/s10765-011-0957-3>.
- Abouelregal, A.E. (2019), "Rotating magneto-thermoelastic rod with finite length due to moving heat sources via Eringen's nonlocal model", *J. Comput. Appl. Mech.*, **50**(1), 118-126. <https://doi.org/10.22059/jcamech.2019.275893.360>.
- Abualnour, M., Chikh, A., Hebali, H., Kaci, A., Tounsi, A., Bousahla, A.A. and Tounsi, A. (2019), "Thermomechanical analysis of antisymmetric laminated reinforced composite plates using a new four variable trigonometric refined plate theory", *Comput. Concrete*, **24**(6), 489-498. <https://doi.org/10.12989/cac.2019.24.6.489>.
- Alzahrani, F.S. and Abbas, I. A. (2016), "The effect of magnetic field on a thermoelastic fiber-reinforced material under GN-III theory", *Steel Compos. Struct.*, **22**(2), 369-386. <https://doi.org/10.12989/scs.2016.22.2.369>.
- Asghar, S., Naeem, M.N., Hussain, M., Taj, M. and Tounsi, A. (2020), "Prediction and assessment of nonlocal natural frequencies of DWCNTs: Vibration analysis", *Comput. Concrete*, **25**(2), 133-144. <https://doi.org/10.12989/cac.2020.25.2.133>.
- Atwa, S.Y. and Jahangir, A. (2014), "Two temperature effects on plane waves in generalized thermo-microstretch elastic solid", *Int. J. Thermophys.*, **35**(1), 175-193. <https://doi.org/10.1007/s10765-013-1541-9>.
- Bakoura, A., Bourada, F., Bousahla, A.A., Tounsi, A., Benrahou, K.H., Tounsi, A., ... Mahmoud, S.R. (2021), "Buckling analysis of functionally graded plates using HSDT in conjunction with the stress function method", *Comput. Concrete*, **27**(1), 73-83. <https://doi.org/10.12989/cac.2021.27.1.073>.
- Balubaid, M., Tounsi, A., Dakhel, B. and Mahmoud, S.R. (2019), "Free vibration investigation of FG nanoscale plate using nonlocal two variables integral refined plate theory", *Comput. Concrete*, **24**(6), 579-586. <https://doi.org/10.12989/cac.2019.24.6.579>.
- Bellifa, H., Benrahou, K.H., Bousahla, A.A., Tounsi, A. and Mahmoud, S.R. (2017), "A nonlocal zeroth-order shear deformation theory for nonlinear postbuckling of nanobeams", *Struct. Eng. Mech.*, **62**(6), 695-702. <https://doi.org/10.12989/sem.2017.62.6.695>.
- Belmahi, S., Zidour, M. and Meradjah, M. (2019), "Small-scale effect on the forced vibration of a nano beam embedded an elastic medium using nonlocal elasticity theory", *Adv. Aircraft. Spacecraft Sci.*, **6**(1), 1-18. <https://doi.org/10.12989/aas.2019.6.1.001>.
- Benahmed, A., Fahsi, B., Benzair, A., Zidour, M., Bourada, F. and Tounsi, A. (2019), "Critical buckling of functionally graded nanoscale beam with porosities using nonlocal higher-order shear deformation", *Struct. Eng. Mech.*, **69**(4), 457-466. <https://doi.org/10.12989/sem.2019.69.4.457>.
- Chen, P.J. and Gurtin, M.E. (1968), "On a theory of heat conduction involving two temperatures", *J. Appl. Math. Phys. (ZAMP)*, **19**, 614-627. <https://doi.org/10.1007/BF01594969>.
- Dhaliwal R.S. and Singh A. (1980), *Dynamic Coupled Thermoelasticity*, Hindustan Publisher Corporation, New Delhi, India.
- Edelen, D.G.B., Green, A.E. and Laws, N. (1971), "Nonlocal continuum mechanics", *Arch. Rat. Mech. Anal.*, **43**, 36-44. <https://doi.org/10.1007/BF00251543>.
- Edelen, D.G.B. and Laws, N. (1971), "On the thermodynamics of systems with nonlocality", *Arch. Rat. Mech. Anal.*, **43**, 24-35. <https://doi.org/10.1007/BF00251543>.
- Eringen, A.C. (2002), *Nonlocal Continuum Field Theories*, Springer, New York, USA.
- Ezzat, M. and El-Barry, A.A. (2017b), "Fractional magneto-thermoelastic materials with phase-lag Green-Naghdi theories", *Steel Compos. Struct.*, **24**(3), 297-307. <https://doi.org/10.12989/scs.2017.24.3.297>.

- Ezzat, M.A. and El-Bary, A.A. (2017a), "A functionally graded magneto-thermoelastic half space with memory-dependent derivatives heat transfer", *Steel Compos. Struct.*, **25**(2), 177-186. <https://doi.org/10.12989/scs.2017.25.2.177>.
- Hussain, M., Naeem, M.N., Tounsi, A. and Taj, M. (2019), "Nonlocal effect on the vibration of armchair and zigzag SWCNTs with bending rigidity", *Adv. Nano Res.*, **7**(6), 431-442. <https://doi.org/10.12989/anr.2019.7.6.431>.
- Jahangir, A., Tanvir, F. and Zenkour, A. (2020), "Reflection of photothermoelastic waves in a semiconductor material with different relaxations", *Ind. J. Phys.*, **95**(1), 51-59. <https://doi.org/10.1007/s12648-020-01690-x>.
- Karami, B., Janghorban, M. and Tounsi, A. (2018), "Nonlocal strain gradient 3D elasticity theory for anisotropic spherical nanoparticles", *Steel Compos. Struct.*, **27**(2), 201-216. <https://doi.org/10.12989/scs.2018.27.2.201>.
- Khan, A.A., Bukhari, S.R., Marin, M. and Ellahi, R. (2019), "Effects of chemical reaction on third-grade MHD fluid flow under the influence of heat and mass transfer with variable reactive index", *Heat Transf. Res.*, **50**(11), 1061-1080. <https://doi.org/10.1615/HeatTransRes.2018028397>.
- Kumar, R., Sharma, N. and Lata, P. (2017), "Effects of Hall current and two temperatures in transversely isotropic magneto-thermoelastic with and without energy dissipation due to ramp-type heat", *Mech. Adv. Mater. Struct.*, **24**(8), 625-635. <https://doi.org/10.1080/15376494.2016.1196769>.
- Lata, P. and Singh, S. (2019), "Effect of nonlocal parameter on nonlocal thermoelastic solid due to inclined load", *Steel Compos. Struct.*, **33**(1), 123-131. <https://doi.org/10.12989/scs.2019.33.1.123>.
- Lata, P. and Singh, S. (2020a), "Deformation in a nonlocal magneto-thermoelastic solid with hall current due to normal force", *Geomech. Eng.*, **22**(2), 109-117. <https://doi.org/10.12989/gae.2020.22.2.109>.
- Lata, P. and Singh, S. (2020b), "Time harmonic interactions in non local thermoelastic solid with two temperatures", *Struct. Eng. Mech.*, **74**(3), 341-350. <https://doi.org/10.12989/sem.2020.74.3.341>.
- Lata, P. and Singh, S. (2020c), "Thermomechanical interactions in a nonlocal thermoelastic model with two temperature and memory dependent derivatives", *Coupl. Syst. Mech.*, **9**(5), 397-410. <https://doi.org/10.12989/csm.2020.9.5.397>.
- Lata, P. and Singh, S. (2020d), "Effects of nonlocality and two temperature in a nonlocal thermoelastic solid due to ramp type heat source", *Arab J. Basic Appl. Sci.*, **27**(1), 358-364. <https://doi.org/10.1080/25765299.2020.1825157>.
- Lata, P. and Singh, S. (2020e), "Plane wave propagation in a nonlocal magneto-thermoelastic solid with two temperature and Hall current", *Wave. Rand. Complex Media*, 1-27. <https://doi.org/10.1080/17455030.2020.1838667>.
- Lata, P. and Singh, S. (2021), "Stoneley wave propagation in nonlocal isotropic magneto-thermoelastic solid with multi-dual-phase lag heat transfer", *Steel Compos. Struct.*, **38**(2), 141-150. <https://doi.org/10.12989/scs.2021.38.2.141>.
- Marin, M. (1996), "Generalized solutions in elasticity of micropolar bodies with voids", *Revista de la Academia Canaria de Ciencias*, **8**(1), 101-106.
- Marin, M., Vlase, S. and Paun, M. (2015), "Considerations on double porosity structure for micropolar bodies", *Aip Adv.*, **5**(3), Art. No. 037113. <https://doi.org/10.1063/1.4914912>.
- Mokhtar, Y., Heireche, H., Bousahla, A.A., Houari, M.S.A, Tounsi, A. and Mahmoud, S.R. (2018), "A novel shear deformation theory for buckling analysis of single layer graphene sheet based on nonlocal elasticity theory", *Smart Struct. Syst.*, **21**(4), 397-405. <https://doi.org/10.12989/sss.2018.21.4.397>.
- Mudhaffar, I.M., Tounsi, A., Chikh, A., Al-Osta, M.A., Al-Zahrani, M.M. and Al-Dulaijan, S.U. (2021), "Hygro-thermo-mechanical bending behavior of advanced functionally graded ceramic metal plate resting on a viscoelastic foundation", *Struct.*, **33**, 2177-2189. <https://doi.org/10.1016/j.istruc.2021.05.090>.
- Othman, M.I. and Abbas, I.A. (2011), "Effect of rotation on plane waves at the free surface of a fibre-reinforced thermoelastic half-space using the finite element method", *Meccanica*, **46**(2), 413-421. <https://doi.org/10.1007/s11012-010-9322-z>.
- Othman, M.I.A. and Abbas, I.A. (2012), "Generalized thermoelasticity of thermal-shock problem in a non-homogeneous isotropic hollow cylinder with energy dissipation", *Int. J. Thermophys.*, **33**, 913-923.

- <https://doi.org/10.1007/s10765-012-1202-4>.
- Refrafi, S., Bousahla, A.A., Bouhadra, A., Menasria, A., Bourada, F., Tounsi, A., ... Tounsi, A. (2020), "Effects of hygro-thermo-mechanical conditions on the buckling of FG sandwich plates resting on elastic foundations", *Comput. Concrete*, **25**(4), 311-325. <https://doi.org/10.12989/CAC.2020.25.4.311>
- Saeed, T., Abbas, I. and Marin, M. (2020), "A GL model on thermo-elastic interaction in a poroelastic material using finite element method", *Symm. Basel*, **12**(3), 1-24, Art. No. 488. <https://doi.org/10.3390/sym12030488>.
- Sharma, N., Kumar, R. and Lata, P. (2016), "Thermomechanical interactions in transversely isotropic magneto-thermoelastic medium with vacuum and with and without energy dissipation with combined effects of rotation, vacuum and two temperatures", *Appl. Math. Model.*, **40**, 6560-6575. <https://doi.org/10.1016/j.apm.2016.01.061>.
- Soleimani, A., Dastani, K., Hadi, A. and Naei, M.H. (2019), "Effect of out of plane defects on the postbuckling behaviour of graphene sheets based on nonlocal elasticity theory", *Steel Compos. Struct.*, **30**(6), 517-534. <https://doi.org/10.12989/scs.2019.30.6.517>.
- Tahir, S.I., Chikh, A., Tounsi, A., Al-Osta, M.A., Al-Dulaijan, S.U. and Al-Zahrani, M.M. (2021), "Wave propagation analysis of a ceramic-metal functionally graded sandwich plate with different porosity distributions in a hygro-thermal environment", *Compos. Struct.*, **269**, 114030. <https://doi.org/10.1016/j.compstruct.2021.114030>.
- Tahir, S.I., Tounsi, A., Chikh, A., Al-Osta, M.A., Al-Dulaijan, S.U. and Al-Zahrani, M.M. (2021), "An integral four-variable hyperbolic HSDT for the wave propagation investigation of a ceramic-metal FGM plate with various porosity distributions resting on a viscoelastic foundation", *Wave. Rand. Complex Media*, 1-24. <https://doi.org/10.1080/17455030.2021.1942310>.
- Youssef, H.M. (2006), "Theory of two-temperature-generalized thermoelasticity", *IMA J. Appl. Math.*, **71**, 383-390. <https://doi.org/10.1093/imamat/hxh101>.
- Youssef, H.M. and Al-Lehaibi, E.A. (2007), "State space approach of two-temperature generalized thermoelasticity of one-dimensional problem", *Int. J. Solid. Struct.*, **44**, 1550-1562. <https://doi.org/10.1016/j.ijsolstr.2006.06.035>.
- Zenkour, A.M. (2020), "Magneto-thermal shock for a fiber-reinforced anisotropic half-space studied with a refined multi-dual-phase-lag model", *J. Phys. Chem. Solid.*, **137**, 109213. <https://doi.org/10.1016/j.jpcs.2019.109213>.
- Zhang, L., Bhatti, M.M., Marin, M. and Mekheimer, K.S. (2020), "Entropy analysis on the blood flow through anisotropically tapered arteries filled with magnetic zinc-oxide (ZnO) nanoparticles", *Entropy*, **22**(10), Art. No.1070. <https://doi.org/10.3390/e22101070>.